

## Modelling of Red Blood Cell Motion and Deformation Using Particle Based Method

Takami Yamaguchi<sup>1</sup>, Yohsuke Imai<sup>2</sup>, and Takuji Ishikawa<sup>3</sup>

**1** Department of Biomedical Engineering,  
Tohoku University  
6-6-01 Aramaki Aza Aoba, Sendai 980-8579, Japan,  
takami@pfs1.mech.tohoku.ac.jp

**3** Department of Bioengineering and Robotics,  
Tohoku University  
6-6-01 Aramaki Aza Aoba, Sendai 980-8579, Japan,  
ishikawa@pfs1.mech.tohoku.ac.jp

**2** Department of Bioengineering and Robotics,  
Tohoku University  
6-6-01 Aramaki Aza Aoba, Sendai 980-8579, Japan,  
yimai@pfs1.mech.tohoku.ac.jp

### Abstract

We have developed a numerical method for simulating micro-scale blood flow. We have applied this method to model blood flow in malaria infection. Our model well simulated the stretching of malaria-infected red blood cells (*Pf*-IRBCs), the deformation of *Pf*-IRBCs in shear flow, and the flow into narrow channels.

We have also investigated the margination of *Pf*-IRBCs in microcirculation.

**Keywords:** Computational biomechanics, Microcirculation, Malaria.

### Introduction

Malaria induced by *Plasmodium falciparum* is one of the most serious infectious diseases on earth. There are about five hundred million clinical cases with two million deaths each year. When a malaria parasite invades and matures within a red blood cell (RBC), the infected RBC (IRBC) becomes stiffer and sticks to healthy RBCs (HRBCs) and endothelial cells (ECs). These changes are postulated to link to microvascular occlusion [1]. Several researchers have investigated cell mechanics of IRBCs using recent experimental techniques, such as micropipette aspiration [2], optical tweezers [3], and microfluidics [4]. These experimental studies are however, still limited to the effect of the single IRBC. Microvascular occlusion may be a hemodynamics problem, involving hydrodynamic and chemical interactions among IRBCs, HRBCs and ECs, but the current experimental techniques have several limitations for this topic. Microvasculature in human body consists of very complex network of circular channels, but we cannot create such complex microchannels for the experiments. It is also difficult to measure the three-dimensional velocity and stress fields simultaneously. Instead, numerical modeling can be a strong tool for further understanding the pathology of malaria. We have developed a numerical model of blood flow in malaria infection [5, 6].

### Method

Blood is a suspension of RBCs in plasma and RBCs consist of cytoplasm enclosed by a thin membrane. Assuming that plasma and cytoplasm are incompressible and Newtonian fluid, the governing equations are described as

$$\frac{D\rho}{Dt} = 0 \quad (1)$$

$$\frac{D\mathbf{u}}{Dt} = -\frac{1}{\rho}\nabla p + \nu\nabla^2\mathbf{u} + \mathbf{f} \quad (2)$$

where the notation  $t$  refers to the time,  $\rho$  is the density,  $\mathbf{u}$  is the velocity vector,  $p$  is the pressure,  $\nu$  is the dynamic viscosity,  $\mathbf{f}$  is the external force per unit mass, and  $D/Dt$  is the Lagrangian derivative.

Our model is based on a particle method. All the components of blood are represented by finite number of particles. Note that each particle is not a real fluid particles but a discrete point for computation. Fluid variables are calculated at the computational point and it is moved by the calculated advection velocity every time step. We use moving particle semi-implicit (MPS) method [7] for solving Eqs. (1) and (2). In micro-scale blood flow simulations, the time step size of time integration is limited by the diffusion number. To avoid the use of small time step size, we employ a fractional

time step method, in which the diffusion and pressure terms are solved by implicit ways.

The membrane of IRBCs and HRBCs are modeled by triangular network of membrane particles. We consider stretch resistance and bending resistance. The force generated by the deformation of membrane is substituted into the force term  $\mathbf{f}$  in Eq. (2) only for membrane particles. The malaria parasite is assumed as a rigid object.

### Stretching of *Pf*-IRBCs

A well known method to quantify the mechanical response of IRBCs is the stretching by the optical tweezers. Suresh et al. [3] measured the axial and transverse diameters of IRBCs at different stages of infection with several stretching forces. Figure 1 shows the comparison between our numerical results and the experimental results for HRBCs, IRBCs at an early stage of infection, ring stage (*Pf*-R-IRBC), and those at the late stage, trophozoite stage (*Pf*-T-IRBC). The numerical results agree well with the experimental results.

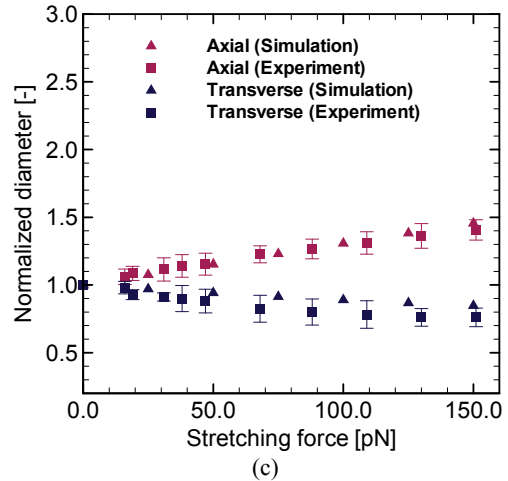
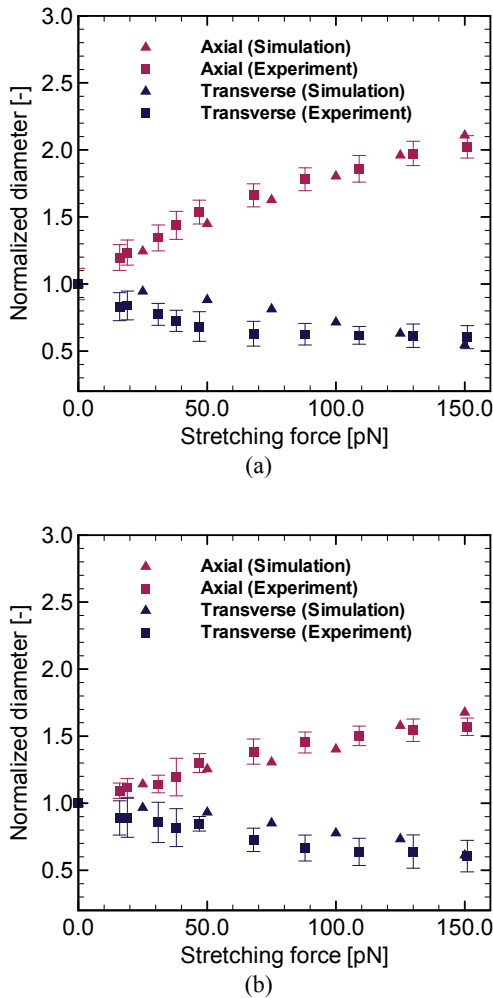


Fig.1 Stretching of *Pf*-IRBCs by optical tweezers: (a) HRBCs; (b) *Pf*-R-IRBCs; (c) *Pf*-T-IRBCs.

### Deformation of *Pf*-IRBCs in Shear Flow

To further validate our model, we examine the deformation of IRBCs in shear flow as shown in Fig. 2. The shear flow, which causes the shear stress of 1.0Pa when there is no RBCs, is given as the flow condition. The ratio of length to width is measured, where the length is the projected one on the shear direction. The length-width ratio is fluctuated in time because the shape of HRBC and IRBCs is not a sphere. Cranston et al. [8] reported that the mean value of the ratio was approximately 1.5 for HRBCs and 1.3 for *Pf*-R-IRBCs in their experiments. The time-averaged values of our results agree well with their results for HRBC and *Pf*-R-IRBC. Cranston et al. did not observe the deformation of *Pf*-T-IRBC, but our model predicts small deformation of it.

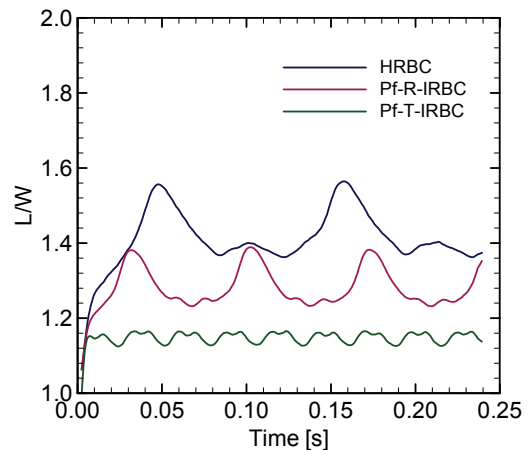


Fig.2 Deformation of *Pf*-IRBCs in shear flow.

### Flow into Narrow Channels

We also simulate the flow into narrow channels using our numerical model. Figure 3 shows snapshots of the numerical simulation for a 4- $\mu$ m-square channel. The HRBC and *Pf*-R-IRBC pass through the narrow channel with large deformation. In contrast, the *Pf*-T-IRBC cannot

enter and occludes the channel, because the deformability of the *Pf*-T-IRBC is lost by following factors: stiffening of the membrane, shape change from biconcave to spherical shape, and the increase of the volume.

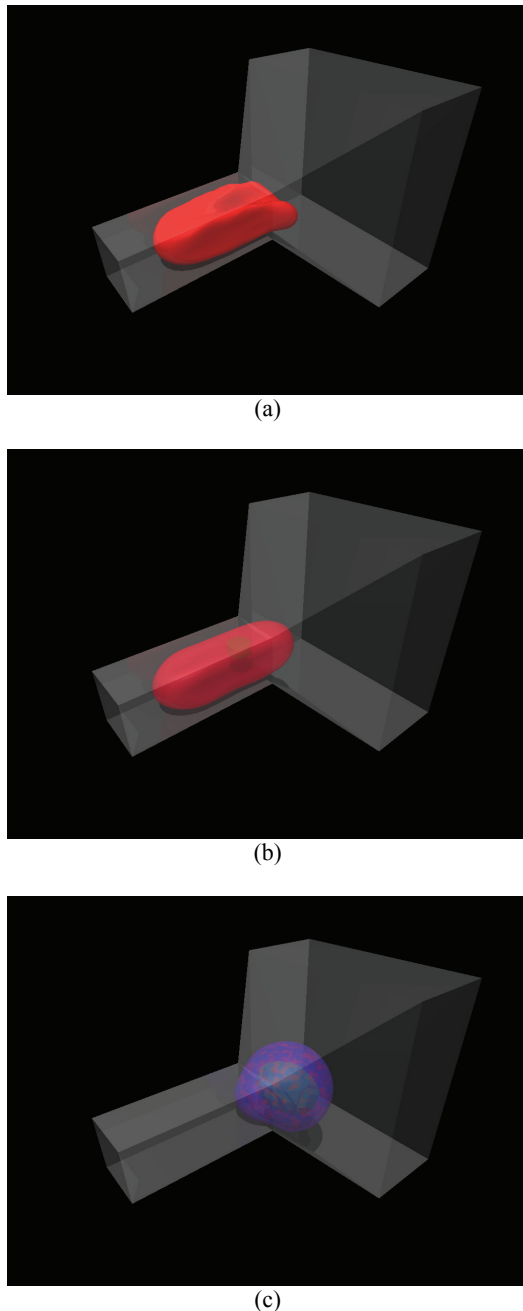


Fig.3 Flow of *Pf*-IRBCs into 4- $\mu$ m-square channel.

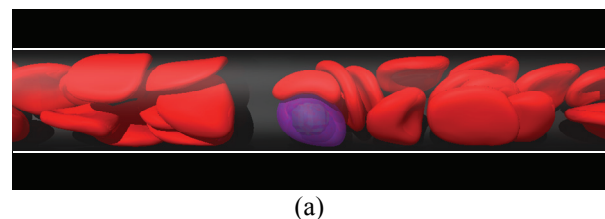
### Margination of *Pf*-IRBCs

We simulate flows in a straight circular channel with a diameter of 12 $\mu$ m to study the margination of *Pf*-IRBCs [9]. The length of the channel is set to be 60 $\mu$ m for the simulation, but the periodic boundary condition is employed to observe long term hemodynamic behavior of RBCs. The flow is driven by the pressure difference between the periodic outlet and inlet so that the mean

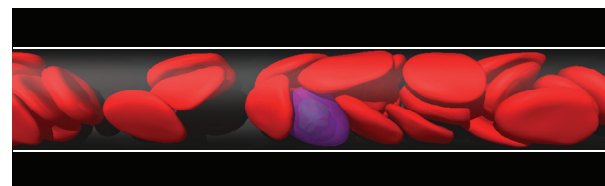
velocity is 1.2 mm/s in the case of healthy blood. In the computational domain (60 $\mu$ m length), we include a *Pf*-T-IRBC and some HRBCs. To study effects of Hct on the margination of *Pf*-T-IRBCs, we compared the flow for two Hct values, Hct = 11% and 27%.

Significant margination is observed in the case of Hct = 27%. Figure 4 shows the typical visualization of the configuration of RBCs for Hct = 27%. Since the velocity of the *Pf*-T-IRBC is lower than HRBCs, the HRBCs catch up and follow the *Pf*-T-IRBC, mimicking "train" formation in the RBCs-leukocyte interaction [10]. One or two HRBCs leading the train lean the *Pf*-T-IRBC, pressing the *Pf*-T-IRBC to the wall of the channel (Fig. 4a), which is also similar to that for leukocytes margination. Since HRBCs in the back are tightly packed, even when one of the leading HRBCs passes away, the next HRBC leans and presses the *Pf*-T-IRBC (Fig. 4b). The continuous interaction results in the margination of the *Pf*-T-IRBC, in which it locates near the wall for a long time period. Figure 5 shows the time histories of the distance between the *Pf*-T-IRBC membrane and the wall surface, where the distance around 0.4 $\mu$ m indicates the contact with the wall because the minimum distance is limited to this value by the spatial resolution of the simulation. The *Pf*-T-IRBC can contact with ECs almost all the time in the high Hct condition.

By contrast, the *Pf*-T-IRBC in Hct = 11% can flow everywhere in the channel as shown in Fig. 5. The *Pf*-T-IRBC and HRBCs form a short train (Fig. 6a), and hence the *Pf*-T-IRBC can marginate and contact instantaneously with ECs in the same interaction manner with the high Hct condition. The interaction however, does not continuously occur in the low Hct condition. The surrounding HRBCs get away from the *Pf*-T-IRBC, and then it immediately comes back to the center of the channel (Fig 6b). The velocity of the axial migration is often faster than single *Pf*-T-IRBC case, because of larger deformation during the interaction. Until when following HRBCs again catch up the *Pf*-T-IRBC, the *Pf*-T-IRBC flows around the center of the channel.



(a)



(b)

Fig.4 Snapshots of RBC flow for Hct = 27%.

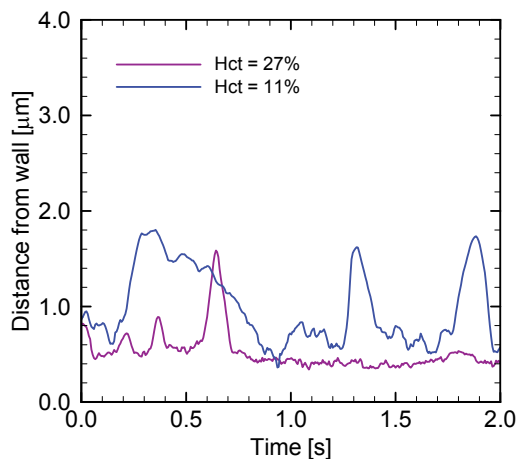


**Fig.5** Time histories of distance between the wall and *Pf*-T-IRBC membrane.

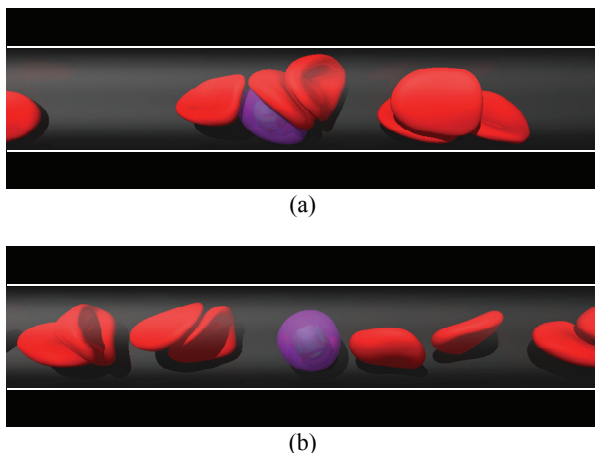


**Fig.6** Snapshots of RBC flow for Hct = 11%.

## Conclusions

We have developed a numerical method for simulating micro-scale blood flow based on a particle method. We have applied this method to model blood flow in malaria infection. Our model well simulated the stretching of malaria-infected red blood cells (*Pf*-IRBCs), the deformation of *Pf*-IRBCs in shear flow, and the flow into narrow channels. We have also investigated the margination of *Pf*-IRBCs in microcirculation. We revealed that continuous interaction between a *Pf*-IRBC and HRBCs is necessary for the margination of the *Pf*-IRBC.

## Acknowledgements

This study was supported by Grant-in-Aid for Scientific Research (S) from the Japan Society for the Promotion of Science (JSPS; No. 19100008), by Grant-in-Aid for Young Scientists (A) from the JSPS (No. 19686016), and by Grant-in-Aid for Young Scientists (B)

from the JSPS (No. 20700373). We also acknowledge the support from the 2007 Global COE Program "Global Nano-Biomedical Engineering Education and Research Network Centre" from the Ministry of Education, Culture, Sports, Science and Technology (MEXT), Japan.

## References

- [1] B.M. Cooke, N. Mohandas, and R.L. Coppel, The malaria-infected red blood cell: structural and functional changes, *Adv. Parasitol.* **26**, pp. 1-86 (2001).
- [2] C.T. Lim, E.H. Zhou and S.T. Quek, Mechanical models for living cells--a review, *J. Biomech.* **39**, pp. 195-216 (2006).
- [3] S. Suresh, J. Spatz, J. P. Mills, A. Micoulet, M. Dao, C.T. Lim M. Beil and T. Seufferlein, Connection between single-cell biomechanics and human disease states: gastrointestinal cancer and malaria, *Acta Biomater.* **1**, pp. 15-30 (2005).
- [4] J.P. Shelby, J. White, K. Ganesan, P.K. Rathod and D.T. Chiu, A microfluidic model for single-cell capillary obstruction by Plasmodium falciparum-infected erythrocytes, *PNAS* **100**, pp. 14618-14622 (2003).
- [5] H. Kondo, Y. Imai, T. Ishikawa, K. Tsubota, and T. Yamaguchi, Hemodynamic analysis of microcirculation in malaria infection, *Ann. Biomed. Eng.* **37**, pp. 702-709 (2009).
- [6] Y. Imai, H. Kondo, T. Ishikawa, C.T. Lim, and T. Yamaguchi, Modeling of hemodynamics arising from malaria infection, *J. Biomech.* **43**, pp. 1386-1393 (2010).
- [7] S. Koshizuka, and Y. Oka, Moving-particle semi-implicit method for fragmentation of incompressible fluid *Nucl Sci Eng* **123**, pp. 421-434 (1996).
- [8] H.A. Cranston, C.W. Boylan, G.L. Carroll, S.P. Sutera, J.R. Williamson, I.Y. Gluzman and D.J. Krogstad, Plasmodium falciparum maturation abolishes physiologic red cell deformability, *Science* **223**, pp. 400-403 (1984).
- [9] Y. Imai, K. Nakaaki, H. Kondo, T. Ishikawa, C.T. Lim and T. Yamaguchi, Margination of red blood cells infected by Plasmodium falciparum in a microvessel, *J. Biomech.* **44**, pp. 1553-1558 (2011).
- [10] G.W. Schmid-Schönbein, S. Usami, R. Skalak, and S. Chien, The interaction of leukocytes and erythrocytes in capillary and postcapillary vessels. *Microvasc. Res.* **19**, pp. 45-70 (1980).